UCLA
UCLA Previously Published Works

Title

Activity and electrochemical properties: iron complexes of the anticancer drug triapine and its analogs

Permalink

https://escholarship.org/uc/item/4nj3k2p0

Journal

JBIC Journal of Biological Inorganic Chemistry, 24(5)

ISSN

0949-8257

Authors

Plamthottam, Sheba
Sun, Daniel
Van Valkenburgh, Juno
et al.

Publication Date

2019-08-01

DOI

10.1007/s00775-019-01675-0

Peer reviewed

Activity and Electrochemical Properties - Iron Complexes of the Anticancer Drug Triapine and Its Analogs

Sheba Plamthottam[1,2], **Daniel Sun**[1,2,‡], **Juno Van Valkenburgh**[1,2,‡], **Jeffrey Valenzuela**[1], **Bastian Ruehle**[1], **Dalton Steele**[1,2], **Soumya Poddar**[2], **Maxim Marshalik**[1], **Selena Hernandez**[1], **Caius Gabriel Radu**[2], **Jeffrey I. Zink**[*,1]

[1]Department of Chemistry, University of California at Los Angeles, Los Angeles, California 90095, United States.

[2]Department of Molecular and Medical Pharmacology, University of California at Los Angeles, Los Angeles, California 90095, United States.

Abstract

Triapine (3-AP), is an iron-binding ligand and anticancer drug that is an inhibitor of human ribonucleotide reductase (RNR). Inhibition of RNR by 3-AP results in the depletion of dNTP precursors of DNA, thereby selectively starving fast-replicating cancer cells of nucleotides for survival. The redox-active form of 3-AP directly responsible for inhibition of RNR is the Fe(II)(3-AP)$_2$ complex. In this work, we synthesize 12 analogs of 3-AP, test their inhibition of RNR *in vitro*, and study the electronic properties of their iron complexes. The reduction and oxidation events of 3-AP iron complexes that are crucial for the inhibition of RNR are modeled with solution studies. We monitor the pH necessary to induce reduction in iron complexes of 3-AP analogs in a reducing environment, as well as the kinetics of oxidation in an oxidizing environment. The oxidation state of the complex is monitored using UV-Vis spectroscopy. Isoquinoline analogs of 3-AP favor the maintenance of the biologically active reduced complex and possess oxidation kinetics that allow redox cycling, consistent with their effective inhibition of RNR seen in our *in vitro* experiments. In contrast, methylation on the thiosemicarbazone secondary amine moiety of 3-AP produces analogs that form iron complexes with much higher redox potentials, that do not redox cycle, and are inactive against RNR *in vitro*.

INTRODUCTION

Metal coordination chemistry plays an important role in the activity of many anticancer drugs. Complexes of platinum, ruthenium, copper, iron, and other metals have been used as successful cancer therapies and have advanced to clinical trials [1, 2]. By tuning the ligand structure and coordination geometries, the redox activity of these complexes can be

controlled [1]. Cisplatin (cis-diamminedichloroplatinum(II)) is one example where reduction potentials and the activity of platinum complexes are dependent on the structure of their ligands. The potency of cisplatin analogs have been enhanced by favoring the more reactive reduced Pt(II) species over the prodrug Pt(IV) species by replacing axial ligands to change the reduction potential [2–4]. Activity of clinical indazole-based ruthenium(III) complexes were enhanced by the electron donor character of the indazole ligands and by tuning their reduction potentials [1, 2, 5, 6]. In the case of platinum and ruthenium complexes, the drug is administered as the coordination complex. In some cases, the free ligand is administered and its activity arises from binding to endogenous metal ions like copper and iron [1, 2]. We see this in the case of the iron-binding heterocyclic thiosemicarbazone Triapine, also known as 3-AP (3-aminopyridine-2-carboxaldehyde thiosemicarbazone), which has become an important drug used in the treatment of cancers [7–14]. This drug is currently undergoing a Phase II clinical trial in the US and has been used in combination therapies to treat acute lymphoblastic leukemia (ALL) in an *in vivo* model [15]. 3-AP works by binding to endogenous iron and forming the reduced iron complex, $Fe(II)(3-AP)_2$, which is directly responsible for inhibition of the enzyme ribonucleotide reductase (RNR), an important target in cancer therapies [16].

Ribonucleotide reductases are a unique class of enzymes known for their unusual free radical mechanism of action. These enzymes reduce ribonucleotides to deoxyribonucleotides, a process essential for DNA replication and repair [17–19]. Inhibitors of RNR are potential drug targets through a mechanism by which they cause nearly complete depletion of dNTP pools, thereby selectively starving fast-replicating cancer cells of nucleotides required for DNA synthesis and replication [15, 20]. Human RNR is composed of two subunits, RRM1 (α_2), the site of nucleotide reduction, and RRM2 (β_2), where a diferric tyrosyl radical cofactor resides (Figure 1a) [16, 18]. *Aye et. al.* used EPR to show that the primary mode of RNR inhibition by 3-AP is donation of an electron by the reduced iron complex of 3-AP, directly quenching the diferric tyrosyl radical on the β_2 subunit (Figure 1b). After this oxidation event, the active $Fe(II)(3-AP)_2$ complex is regenerated by reducing agents in the cell. This redox cycling has been found to be necessary for the continued inhibition of RNR [16, 21–23].

3-AP is an α-N-heteroyclic carboxaldehyde thiosemicarbazone (HCT), which are a broad class of metal-binding redox agents that have been studied as far back as the 1940's. A variety of HCT analogs have been synthesized. Over the past 70 years, modifications to 3-AP have yielded compounds that appear structurally similar but may display unique redox properties related to their metal binding properties and their interactions with their clinical target, ribonucleotide reductase [22, 24, 25]. French and Sartorelli groups developed many 3-AP analogs with the pyridine scaffold [7, 26, 27]. Compounds that have substitutions on the H atom of the secondary amine have been shown to be biologically inactive, however it is unclear why this modification results in inactive complexes [28]. Additionally, French reported a distinct set of compounds that showed promising activity, in which the pyridine ring was replaced by an isoquinoline [29].

Molecular docking experiments on mouse R2 RNR have shown that the pyridine ring of 3-AP is stabilized by hydrophobic residues phenylalanine, serine, and tyrosine in the active

pocket. Hydrogen bonding by amine groups on 3-AP with glutamate, aspartate, and arginine residues in the active site have also shown to stabilize the interaction. Particularly, the amino group on the pyridine ring is stabilized by a glutamic acid residue in the pocket [30]. Removal of this amine has shown to decrease activity of 3-AP 5-fold [24]. Particular isoquinoline analogs of 3-AP have been found to have improved activity, despite losing this interaction. This result is difficult to explain with known active site binding interactions. Additionally, studies done on heavily substituted isoquinoline analogs of 3-AP have shown that bulky groups may not be well tolerated in the active site, but the activity of minimally-substituted isoquinoline analogs remains difficult to explain [31].

Although these isoquinoline compounds were shown to possess higher anticancer activity than 3-AP, the effects of the ligand on the electrochemical properties of the iron complex have not been explored. It has been shown that formation of the $Fe(II)(3-AP)_2$ complex is essential for the inhibitory effect of the drug 3-AP, while the Fe(III) complex of 3-AP is inactive [16]. In this work, 3-AP drug analogs are made in-house, and using spectroscopic methods, we investigate the stability of Fe(II) complexes in a reducing environment, the oxidation rates of the analog complexes, as well as use electrochemical studies to determine their redox potentials. These findings help us understand how structural modifications to 3-AP affect the electronic structure of their iron complexes, and subsequently their biological activity.

RESULTS AND DISCUSSION

Structure of ligands and biological activity.

3-AP is a potent and fast-acting RNR inhibitor *in vitro* [32–34]. Treatment of cells by 3-AP inhibits conversion of ribonucleotide diphosphates to deoxyribonucleotides diphosphates, thereby inhibiting DNA synthesis. S-phase arrest is a characteristic phenotype of cells treated with 3-AP [15]. The three classes of 3-AP analogs in Figure 2 are grouped by their structure and biological activity. IC_{50} values (Figure 3a) and S-phase arrest (Figure 3b) of the analogs in MIA PaCa-2 PDAC (pancreatic ductal adenocarcinoma) cells are determined after 72h and 24h treatment, respectively. Group I compounds are all methylated on the secondary amine and show no RNR-specific activity. All the analogs except for the Group I compounds induce S-phase arrest in the concentration range of 250 nM to 5 μM. Group II compounds are the most structurally similar to 3-AP, and their iron complexes, as will be shown later, are the most spectroscopically similar to 3-AP with non-aromatic modifications made either on the left or the right side of the scaffold. Group II-A compounds have non-aromatic substituents on the pyridine ring (TS-1, TS-2, and TS-3), while Group II-B compounds have substituents to the primary amine part of the thiosemicarbazone moiety (DS-1, DS-2, and DS-3). Group II-B compounds have similar IC_{50} values to 3-AP (1 μM), with DS-3 (470 nM) being slightly more potent than 3-AP, while Group II-A compounds are all less potent (IC_{50} values 1.7–3 μM). In Group III compounds, the pyridine ring of 3-AP was replaced with isoquinolines (IQ-1, IQ-2, and IQ-3). Consistent with enzyme inhibition studies, which showed that isoquinoline analogs exhibit potent inhibition of RNR [31], we find that Group III compounds inhibit cell proliferation at similar or lower concentrations (250 nM-0.7 μM) than 3-AP, with IQ-2 being four-fold more potent than 3-AP (250 nM). As

will be discussed later, each class of compounds forms iron complexes with unique UV-Vis spectral and redox properties. In addition, their iron complexes share some spectral commonalities by UV-Vis that allow to develop spectroscopic assays to probe activity of the biologically active iron complex.

Absorption spectra.

3-AP and analogs that contain the pyridine ring display two absorption bands in the in the UV-Vis between 260 and 450 nm corresponding to n→pi* and pi→pi* transitions (Figure 4 and Figure S1). Their iron(II) and iron(III) complexes have distinct absorbances. Figure S1 shows UV-spectra for iron(II) titrations of all 12 compounds. Upon complexation with Fe(II) and Fe(III), the 3-AP complexes display peaks in the 400–500 nm region characteristic of charge transfers, while only the Fe(II) complexes display metal-to-ligand charge transfer transitions (MLCT) in the visible region between 590–630 nm (Figure 4b). These lowest energy bands are very intense with molar absorptivities on the order of 3000–9000 $M^{-1}cm^{-1}$ (Figure 5b) and were thus assigned to be charge transfer transitions in the reduced complex. The wavelength of the lowest energy metal-to-ligand charge transfer transitions are characteristic to each class of compounds, where complexes of Group I compounds are blue-shifted while that of the Group III compounds are red-shifted relative to 3-AP (Figure 5a).

DFT calculations support that the iron(II) complexes undergo MLCT. The HOMO of the 3-AP iron(II) complex shows strong pi antibonding interactions with d-orbitals of the iron center (Figure 6b). The LUMO has strong ligand character, with electron density distributed throughout the pi system and strongly localized on the secondary amine on the thiosemicarbazone backbone (Figure 6c). The reduced form of the 3-AP iron complex was determined to be the active species involved in β_2 inhibition [16], and the lowest energy transitions of the reduced complexes tell us important features about their oxidation mechanism. This charge transfer peak, which is only present in the Fe(II) complex, can be used to track the stability of the Fe(II) 3-AP analog complexes.

Stability of the Fe(II) species in a reducing environment.

To be an active inhibitor of RNR, the 3-AP iron complex has to (1) get reduced to the Fe(II) form in the reducing environment of the cell, and (2) undergo oxidation to quench the tyrosyl radical in the enzyme active site. To test these two properties, we designed two distinct solution studies to look closer at the reduction of the Fe(III) complex and the oxidation of the Fe(II) complex. For the first, UV-Vis spectroscopic pH titrations were used to monitor the effect of pH on the stability of the iron(II) complexes in a reducing environment. Cells are reducing environments which contain species such as glutathione and NADH that allow redox cycling of iron complexes [35]. Per its mechanism of action, the 3-AP iron complex must get reduced in order for it to be in its active form. We used a model system to mimic the reduction of the iron(III) complex in the reducing environment of the cell. There is a pH dependence on the stability of the active Fe(II) species with different ligands (Figure 7). The pH dependence may likely be due to protonation and ligand dissociation or oxidation.

Most of the Fe(II) complexes stay in their active form at pH values 6.1–6.8. However, the most drastic differences are seen in the Group III isoquinoline series (compounds IQ-1, IQ-2, and IQ-3), where their reduced complexes are stable at pH 2.9–4.0. There is an increased stability of the Fe(II) complexes over a broad pH range with the isoquinoline ligands, which is consistent with their increased activity against RNR. Surprisingly, despite their lack of activity, the Group I methylated series (compounds MS-1, MS-2, MS-3) also form stable reduced complexes at low pH values. Although MS compounds form stable reduced complexes, kinetics data about their oxidation may explain their inactivity against RNR.

Spectroscopic methods were then used to calculate the half-life of the reduced complexes t_{50}, the time taken for 50% of the complex to get oxidized under the given experimental conditions (Figure 8). Compounds fall into three groups: non-oxidizers with no RNR-specific activity, fast oxidizers with low activity, and slow oxidizers with the greatest activity. Iron(II) complexes of the Group I ligands, MS-1, MS-2, and MS-3, which are inactive *in vitro*, do not get oxidized over the time frame of the experiment and stay in their reduced form for days. Group II-A compounds, with non-aromatic modifications on the left side (compounds TS-1, TS-2, and TS-3), form complexes that get oxidized faster than the 3-AP iron complex and are less potent RNR inhibitors (Figure 3). Addition of electron donating groups to the right side of the 3-AP scaffold (compounds DS-1, DS-2, and DS-3) results in similar maintenance of their reduced complex and are potent RNR inhibitors. The iron(II) complexes of the Group III ligands get oxidized slowly and are two to four times more potent than 3-AP *in vitro*.

Reduction potentials and trends.

Cyclic voltammetry was used to determine the reduction potential of 3-AP analog complexes. It is noted that complexes that get reduced over a broad pH range and are slow to oxidize have higher redox potentials. Group III IQ compounds form stable reduced complexes consistent with their higher redox potentials, whereas Group II compounds form less stable reduced complexes and have lower redox potentials.

The increased stability of the reduced complex by isoquinoline ligands can be explained by their increased ligand strength. In the spectrochemical series, stronger ligands cause more d-orbital splitting. Isoquinolines act as strong Lewis bases and pi-acceptor ligands, which tend to interact strongly with orbitals of transition metals to cause large splitting of d-orbital energies. Assuming low spin d^5 and d^6 complexes, as have been described for complexes of Triapine [36–39], larger d-orbital splitting increases the CFSE of d^6 complexes relative to d^5 ones, and would thus increase the redox potential of their complexes. Cyclic voltammetry was used to measure the reduction potential and found that the Group III isoquinoline complexes indeed had higher reduction potentials (Figure 9–10). Group III compounds are still able to get oxidized, but their potentials are still not out of the range of the cellular environment.

The higher reduction potentials of the Group III complexes are consistent with the isoquinoline ligand's ability to stabilize the Fe(II) form. Adding conjugation on the pyridine ring of 3-AP, as in the case of the Group III series, increases sigma donation from the lone

pair of the sp^2-hybridized pyridine nitrogen making isoquinoline ligands, IQ-1, IQ-2, and IQ-3, stronger Lewis bases than 3-AP. In turn, these modifications increase the pi-accepting character of the ligand and favor the biologically active Fe(II) form of the complex. Furthermore, the long half-life required for oxidation of the Group III complexes is consistent with their ability to favor the Fe(II) form, as well as is their stability over a wider pH range.

An interesting case is that of complexes having redox potentials that are "too high." It is evidenced in the case of the Group I compounds, MS-1, MS-2, and MS-3, which have high redox potentials outside the range of the cellular environment (Figure 10), are unable to redox cycle, and do not induce S-phase arrest of cells after 24-hour treatment *in vitro*. The mechanism of RNR inhibition requires donation of an electron from the reduced Fe(II) complex to a tyrosyl radical [16]. Redox potentials of the active 3-AP complexes need to be in the range of the cellular environment to inhibit RNR, because electron donation, i.e. oxidation of the iron complex, is ultimately required for inhibition. Furthermore, redox cycling is required for maintaining the function of the drug. Besides Group I complexes, all the other complexes we tested have potentials in the range of the cellular environment.

CONCLUSIONS

There are other contributing factors that modulate activity of the 3-AP analogs against RNR such as cell uptake, solubility, and chemical stability of the ligand in a biological environment. However, the present studies give an understanding of the electronic components of what makes a potent 3-AP analog. To be an active inhibitor of RNR, the 3-AP iron complex has to (1) get reduced to the Fe(II) form in the reducing environment of the cell, and (2) undergo oxidation to quench the tyrosyl radical in the enzyme active site. To test these two properties, we designed two distinct solution studies to look closer at the reduction of the Fe(III) complex and the oxidation of the Fe(II) complex. Oxidation rates of the 3-AP analog Fe(II) complexes have shown to be a useful indicator of potency of the analogs *in vitro*. Oxidation rate can be determined from the decrease in the lowest energy charge transfer peak using UV-Vis spectroscopy. Due to its simplicity, this method has the potential to be used in a microplate assay with UV absorption-detection to quickly screen potential drug candidates.

Reduction potentials are also a good indicator of biological activity, where the most potent compounds have iron complexes with reduction potentials below 0.2 V, within the range of the cellular environment, so that the complex can undergo oxidation per its mechanism of action. The unique mechanism of RNR inhibition requires that the 3-AP iron complex be able to cycle between the reduced and oxidized forms. Like the ruthenium complexes, we find that there is a narrow redox window [1, 2, 5, 6] to which the complexes are active. Methylation on the secondary amine of the thiosemicarbazone drastically alters the reduction potential (greater than 0.5 V), causing non-specific activity of the drug, in the case of the methylated Group I complexes. Group III-type isoquinoline modifications to the 3-AP scaffold have the potential to improve the potency of RNR inhibitors. They are an example of structural modifications to 3-AP that form iron complexes with adequate redox potentials,

allow for redox cycling, favor the biologically active Fe(II) species, and thereby improve the potency of 3-AP *in vitro*.

EXPERIMENTAL SECTION

Materials.

Ammonium iron (II) sulfate hexahydrate (Sigma Aldrich), iron(III) nitrate nonahydrate (Alfa Aesar), Dimethyl sulfoxide (Sigma Aldrich), L-dithiothreitol (DTT) (Sigma Aldrich) were used as received. Potassium chloride (KCl) (Sigma) was recrystallized three times from water before use. Glassy Carbon and Ag/AgCl Reference Electrodes were obtained from CHI Instruments.

Synthesis of 3-AP analogs.

Please see Supplemental Information File for synthesis and characterization data (^{1}H-NMR, ^{13}C-NMR, and HPLC).

Synthesis of Iron(II) and (III) complexes.

100 mM stock solutions of Fe(II) and Fe(III) salts are made in degassed 18 megohm water. 10 mM 3-AP analog stocks are made in DMSO. Iron salt solution is added to the ligand solution at a molar ratio of 1:2 (Fe:3-AP). Upon addition of the iron salt, the bis-complex Fe(3-AP)$_2$ forms readily in solution and a color change follows [16, 21]. The iron(III) complexes are quite stable, but the iron(II) compounds need to be degassed and stored under argon to prevent oxidation. 3-AP analogs have very low solubility in buffers and low solubility in water. For UV-Vis experiments, complexes are made and used at concentrations 100 μM-300μM. All UV-Vis measurements are done on a Varian Cary 5000 UV-Vis-NIR Spectrophotometer.

Cell culture conditions.

Human cell line MIA PaCa-2 (pancreatic ductal adenocarcinoma) was obtained from American Type Culture Collection and maintained in 10% FBS in DMEM, and were cultured at 37°C, 20% O$_2$ and 5% CO$_2$. The cultures were regularly tested for mycoplasma contamination using MycoAlert kit (Lonza) following manufacturer's instructions.

Cell proliferation assay.

Cells were plated in 384-well plates (500 cells/well in 30 μL volume). Drugs were serially diluted to desired concentrations and an equivalent volume of DMSO was added to vehicle control. 10 μL of the 4× diluted drugs were added to each well. Following 72 h incubation, ATP content was measured using CellTiter-Glo reagent according to manufacturer's instructions (Promega, CellTiter-Glo Luminescent Cell Viability Assay), and analyzed by SpectraMax luminometer (Molecular Devices). IC$_{50}$ values, concentrations required to inhibit proliferation by 50% compared to DMSO treated cells, were calculated using Prism 6.0 h (Graphpad Software).

FACS analysis of S-phase arrest.

250,000 MIA PaCa-2 cells were seeded per well in a 12-well plate. The cells were treated with indicated compounds for 24 hours. The cells were trypsinized and spun down at 450 × g for 5 min, washed with PBS twice, and resuspended in 300 μL Propidium iodide solution (containing Ribonuclease A and 0.3% Triton X-100). The samples were protected from light before acquisition by flow cytometry. All flow cytometry data were acquired on a five-laser LSR FORTESSA or LSRII (BD), and analyzed using the FlowJo software (Tree Star).

Energy transitions of 3-AP analog complexes.

Extinction coefficients of the reduced complexes' lowest energy transition are calculated using the Beer-Lambert Law from the maximum absorbance of the 2:1 species.

Iron titrations 3-AP analogs: calculating relative K_a's.

A spectroscopic Fe(II) binding assay, in which the drug is titrated with Fe(II) under argon such that the rate of oxidation is negligible. Iron and drug solutions are degassed for 10 min before the titration. The absorbance of the metal complex's charge transfer peak at ~600 nm is plotted against the equivalents of iron added, and the Beer-Lambert law is applied to determine the extinction coefficient of the complex at that wavelength.

10 mM stock solutions of drug are made in DMSO. All titrations are done with 3 mL of 100 μM drug in water (1% DMSO). To keep the volume change <10%, 7.5 μL of 2.5 mM ammonium iron (II) sulfate in water is added to get each spectrum (16 times). Then 15 μL is added (8 times). For iron(III) titrations, iron(III) nitrate nonahydrate is used as the iron source.

pH titrations.

Spectroscopic pH titrations are used to monitor the effect of pH on the reduction of the iron(III) complexes in the presence of the reducing agent DTT. 3-AP analog Fe(III) complexes are synthesized as described previously. Briefly, 1 equivalent of iron(III) nitrate nonahydrate (solution in water) is added to 2 equivalents of 3-AP (stock in DMSO) to make a 100 uM solution of metal complex in water. DTT is added to this solution for a final concentration of 500 nM – 1 mM DTT. Complex is titrated with a triethylamine/water solution and pH is measured every 0.2–0.5 pH units. Complexes are titrated between pH 3.2 to 9. The starting point of the titration is the pH of the initial ligand solution, which ranges from pH 3.2–5.0, depending on the ligand. The appearance of the charge transfer peak at 600 nm, which is only present in the iron (II) complexes, is used to monitor the stability of the reduced Fe(II)(3-AP)$_2$ complexes after the addition of 500 nM-1 mM DTT. The end point of the titration is determined by a plateau of the absorbance at the 600 nm charge transfer peak. The pH at which 50% of the complex is in the bis-Fe(II) form is calculated using a sigmoidal dose-response fitting in Origin Pro 9.1. Changing the pH alone without the reducing agent does not affect the reduction of the complexes. Spectra are taken after solutions have reached equilibrium. Note that reduction of the Fe(III) complexes occur <1 min, whereas oxidation is slower.

Oxidation rate of Fe(II) complexes.

Iron(II) complexes of 3-AP analogs are made at 2:1 ratio of ligand:Fe(II) salt under argon. The charge transfer peak that is only present in the reduced form of the complex is used to monitor the rate of oxidation of the iron (II) complex over time. The oxidation rate of Fe(II) (3-AP)$_2$ is plotted as a function of the absorbance at the ~600 nm peak vs time. T$_{50}$, the time it takes for 50% of the complex to get oxidized under the given experimental conditions, is calculated for all the 3-AP analog complexes.

Cyclic voltammetry (CV).

CV experiments are carried out under argon. 0.1 M KCl is used as the electrolyte solution. Due to solubility limitations, all compounds are dissolved in 30% DMSO/0.1 M KCl at 2 mM. The bis-complexes are made *in situ* by addition of ammonium iron (II) sulfate hexahydrate, where final Fe concentration is 1 mM. The following parameters are used to acquire the voltammograms. Scan rate: 0.1 V/s, sensitivity 10^{-6}, reference electrode: Ag/AgCl, auxiliary and working electrode: glassy carbon.

Density Functional Theory calculations.

DFT calculations are done using Gaussian09. Crystal structure for Fe(III)(3-AP)$_2$ from Kowol et al. is used as the starting point for geometry optimizations of the 3-AP complex [24]. DFT, B3LYP, 6–31+G* basis set is used for geometry optimization. The SDD basis set is used for Fe^{2+} and 6–31+G* is used for H, C, N, S, and O. Single point energy calculations are done using a larger basis set (6–31+G**), with zero-point corrections from the converged frequency file.

Supplementary Material

Refer to Web version on PubMed Central for supplementary material.

ACKNOWLEDGMENT

REFERENCES

1. Graf N, Lippard SJ (2012) Redox activation of metal-based prodrugs as a strategy for drug delivery. Adv Drug Deliv Rev 64:993–1004. 10.1016/j.addr.2012.01.007 [PubMed: 22289471]

2. Reisner E, Arion VB, Keppler BK, Pombeiro AJL (2008) Electron-transfer activated metal-based anticancer drugs. Inorganica Chim Acta 361:1569–1583. 10.1016/j.ica.2006.12.005

3. Bruijnincx PC, Sadler PJ (2008) New trends for metal complexes with anticancer activity. Curr Opin Chem Biol 12:197–206. 10.1016/j.cbpa.2007.11.013 [PubMed: 18155674]

4. Alderden RA, Hall MD, Hambley TW (2009) The Discovery and Development of Cisplatin. J Chem Educ 83:728 10.1021/ed083p728

5. Clarke MJ (2002) Ruthenium metallopharmaceuticals. Coord Chem Rev 232:69–93. 10.1016/S0010-8545(02)00025-5

6. Galanski M, Arion V, Jakupec M, Keppler B (2003) Recent Developments in the Field of Tumor-Inhibiting Metal Complexes. Curr Pharm Des 9:2078–2089. 10.2174/1381612033454180 [PubMed: 14529417]
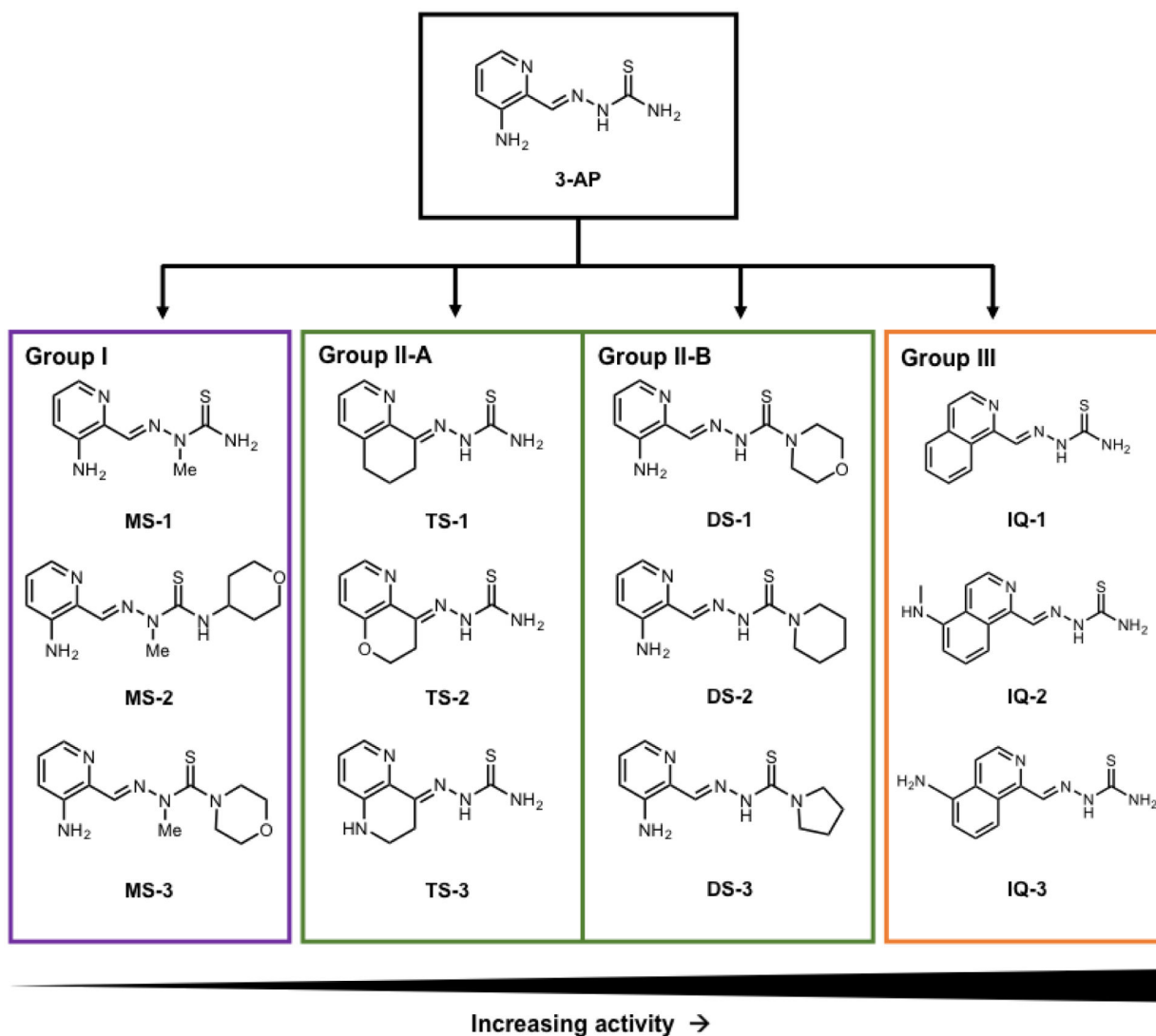
7. Liu M-C, Lin T-S, Cory JG, et al. (1996) Synthesis and Biological Activity of 3- and 5-Amino Derivatives of Pyridine-2-carboxaldehyde Thiosemicarbazone. J Med Chem 39:2586–2593. 10.1021/jm9600454 [PubMed: 8691457]

8. Cory JG, Cory AH, Rappa G, et al. (1995) Structure-function relationships for a new series of pyridine-2-carboxaldehyde thiosemicarbazones on ribonucleotide reductase activity and tumor cell growth in culture and in vivo. Adv Enzyme Regul 35:55–68. 10.1016/0065-2571(94)00005-N [PubMed: 7572354]

9. Finch RA, Liu M-C, Cory AH, et al. (1999) Triapine (3-aminopyridine-2-carboxaldehyde thiosemicarbazone; 3-AP): an inhibitor of ribonucleotide reductase with antineoplastic activity. Adv Enzyme Regul 39:3–12. 10.1016/S0065-2571(98)00017-X [PubMed: 10470363]

10. Dai L, Lin Z, Qiao J, et al. (2017) Ribonucleotide reductase represents a novel therapeutic target in primary effusion lymphoma. Oncogene 36:5068–5074. 10.1038/onc.2017.122 [PubMed: 28459467]

11. Cory JG, Cory AH, Rappa G, et al. (1994) Inhibitors of ribonucleotide reductase. Biochem Pharmacol 48:335–344. 10.1016/0006-2952(94)90105-8 [PubMed: 8053929]

12. Finch RA, Liu MC, Grill SP, et al. (2000) Triapine (3-aminopyridine-2-carboxaldehyde-thiosemicarbazone): A potent inhibitor of ribonucleotide reductase activity with broad spectrum antitumor activity. Biochem Pharmacol 59:983–991. 10.1016/S0006-2952(99)00419-0 [PubMed: 10692563]

13. Nutting CM, Van Herpen CML, Miah AB, et al. (2009) Phase II study of 3-AP Triapine in patients with recurrent or metastatic head and neck squamous cell carcinoma. Ann Oncol 20:1275–1279. 10.1093/annonc/mdn775 [PubMed: 19246715]

14. Traynor AM, Lee J-W, Bayer GK, et al. (2010) A phase II trial of Triapine (NSC# 663249) and gemcitabine as second line treatment of advanced non-small cell lung cancer: Eastern Cooperative Oncology Group Study 1503. Invest New Drugs 28:91–97. 10.1007/s10637-009-9230-z [PubMed: 19238328]

15. Le TM, Poddar S, Capri JR, et al. (2017) ATR inhibition facilitates targeting of leukemia dependence on convergent nucleotide biosynthetic pathways. Nat Commun 8:. 10.1038/s41467-017-00221-3

16. Aye Y, Long MJC, Stubbe J (2012) Mechanistic studies of semicarbazone triapine targeting human ribonucleotide reductase in vitro and in mammalian cells: Tyrosyl radical quenching not involving reactive oxygen species. J Biol Chem 287:35768–35778. 10.1074/jbc.M112.396911 [PubMed: 22915594]

17. Mathews CK (2016) The Most Interesting Enzyme in the World. Structure 24:843–844. 10.1016/j.str.2016.05.006 [PubMed: 27276424]

18. Uhlin U, Eklund H (1994) Structure of ribonucleotide reductase protein R1. Nature 370:533–539. 10.1038/370533a0 [PubMed: 8052308]

19. Nordlund P, Reichard P (2006) Ribonucleotide Reductases. Annu Rev Biochem 75:681–706. 10.1146/annurev.biochem.75.103004.142443 [PubMed: 16756507]

20. Aird KM, Zhang R (2015) Nucleotide metabolism, oncogene-induced senescence and cancer. Cancer Lett. 356:204–210 [PubMed: 24486217]

21. Richardson DR, Kalinowski DS, Richardson V, et al. (2009) 2-Acetylpyridine Thiosemicarbazones are Potent Iron Chelators and Antiproliferative Agents: Redox Activity, Iron Complexation and Characterization of their Antitumor Activity. J Med Chem 52:1459–1470. 10.1021/jm801585u [PubMed: 19216562]

22. Enyedy ÉA, Nagy NV, Zsigó É, et al. (2010) Comparative Solution Equilibrium Study of the Interactions of Copper(II), Iron(II) and Zinc(II) with Triapine (3-Aminopyridine-2-carbaldehyde Thiosemicarbazone) and Related Ligands. Eur J Inorg Chem 2010:1717–1728. 10.1002/ejic.200901174

23. Enyedy É a, Primik MF, Kowol CR, et al. (2011) Interaction of Triapine and related thiosemicarbazones with iron(III)/(II) and gallium(III): a comparative solution equilibrium study. Dalton Trans 40:5895–905. 10.1039/c0dt01835j [PubMed: 21523301]

24. Kowol CR, Trondl R, Heffeter P, et al. (2009) Impact of metal coordination on cytotoxicity of 3-aminopyridine-2- carboxaldehyde thiosemicarbazone (Triapine) and novel insights into terminal dimethylation. J Med Chem 52:5032–5043. 10.1021/jm900528d [PubMed: 19637923]

25. Pelosi G (2010) Thiosemicarbazone Metal Complexes: From Structure to Activity. Open Crystallogr J 3:16–28. 10.2174/1874846501003020016

26. Antholine WE, Knight JM, Petering DH (1976) Inhibition of tumor cell transplantability by iron and copper complexes of 5-substituted 2-formylpyridine thiosemicarbazones. J Med Chem 19:339–341. 10.1021/jm00224a030 [PubMed: 1249818]

27. Wallace R, Richard Thomson J, Bell MJ, Skipper HE (1956) Observations on the Antileukemic Activity of Pyridine- 2-carboxaldehyde Thiosemicarbazone and Thiocarbohydrazone. Cancer Res 16:167–170 [PubMed: 13293659]

28. Agrawal KC, Sartorelli AC (1969) Potential antitumor agents. II. Effects of modifications in the side chain of 1-formylisoquinoline thiosemicarbazone. J Med Chem 12:771–774. 10.1021/jm00305a011 [PubMed: 5812185]

29. French FA, Blanz EJ (1965) The Carcinostatic Activity of α-N Heterocyclic Carboxaldehyde Thiosemicarbazones. Cancer Res 25:1454–1458 [PubMed: 5862990]

30. Popovi -Bijeli A, Kowol CR, Lind MES, et al. (2011) Ribonucleotide reductase inhibition by metal complexes of Triapine (3-aminopyridine-2-carboxaldehyde thiosemicarbazone): A combined experimental and theoretical study. J Inorg Biochem 105:1422–1431. 10.1016/j.jinorgbio.2011.07.003 [PubMed: 21955844]

31. Mooney PD, Booth BA, Moore EC, et al. (1974) Potential antitumor agents. Synthesis and biochemical properties of 5-N-alkylamino-, N,N-dialkylamino-, and N-alkylacetamido-1-formylisoquinoline thiosemicarbazones. J Med Chem 17:1145–1150. 10.1021/jm00257a004 [PubMed: 4370274]

32. Lin ZP, Belcourt MF, Carbone R, et al. (2007) Excess ribonucleotide reductase R2 subunits coordinate the S phase checkpoint to facilitate DNA damage repair and recovery from replication stress. Biochem Pharmacol 73:760–772. 10.1016/j.bcp.2006.11.014 [PubMed: 17188250]

33. Buss Joan L., Greene Bryan T., Turner JoLyn, et al. (2005) Iron Chelators in Cancer Chemotherapy. Curr Top Med Chem 4:1623–1635. 10.2174/1568026043387269

34. Yu Y, Wong J, Lovejoy DB, et al. (2006) Chelators at the Cancer Coalface: Desferrioxamine to Triapine and Beyond. Clin Cancer Res 12:6876–6883. 10.1158/1078-0432.CCR-06-1954 [PubMed: 17145804]

35. Kappus H (1986) Overview of enzyme systems involved in bioreduction of drugs and in redox cycling. Biochem Pharmacol 35:1–6. 10.1016/0006-2952(86)90544-7

36. Popovi -Bijeli A, Kowol CR, Lind MES, et al. (2011) Ribonucleotide reductase inhibition by metal complexes of Triapine (3-aminopyridine-2-carboxaldehyde thiosemicarbazone): A combined experimental and theoretical study. J Inorg Biochem 105:1422–1431. 10.1016/j.jinorgbio.2011.07.003 [PubMed: 21955844]

37. Bernhardt PV, Sharpe PC, Islam M, et al. (2009) Iron chelators of the dipyridylketone thiosemicarbazone class: Precomplexation and transmetalation effects on anticancer activity. J Med Chem 52:407–415. 10.1021/jm801012z [PubMed: 19090766]

38. Kolesar JM, Schelman WR, Geiger PG, et al. (2008) Electron paramagnetic resonance study of peripheral blood mononuclear cells from patients with refractory solid tumors treated with Triapine. J Inorg Biochem 102:693–698. 10.1016/j.jinorgbio.2007.10.013 [PubMed: 18061679]

39. Pelivan K, Miklos W, Van Schoonhoven S, et al. (2016) Differences in protein binding and excretion of Triapine and its Fe(III) complex. J Inorg Biochem 160:61–69. 10.1016/j.jinorgbio.2015.10.006 [PubMed: 26507768]

a

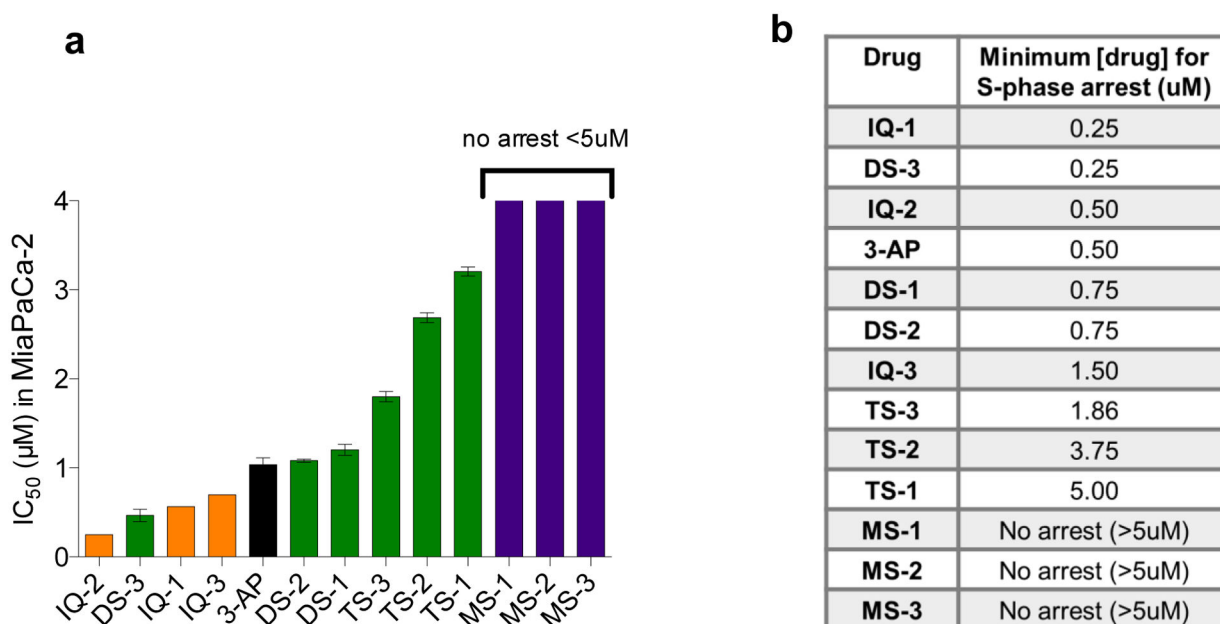**Ribonucleotide Reductase (RNR)**

RRM1

Active site

RRM2

b
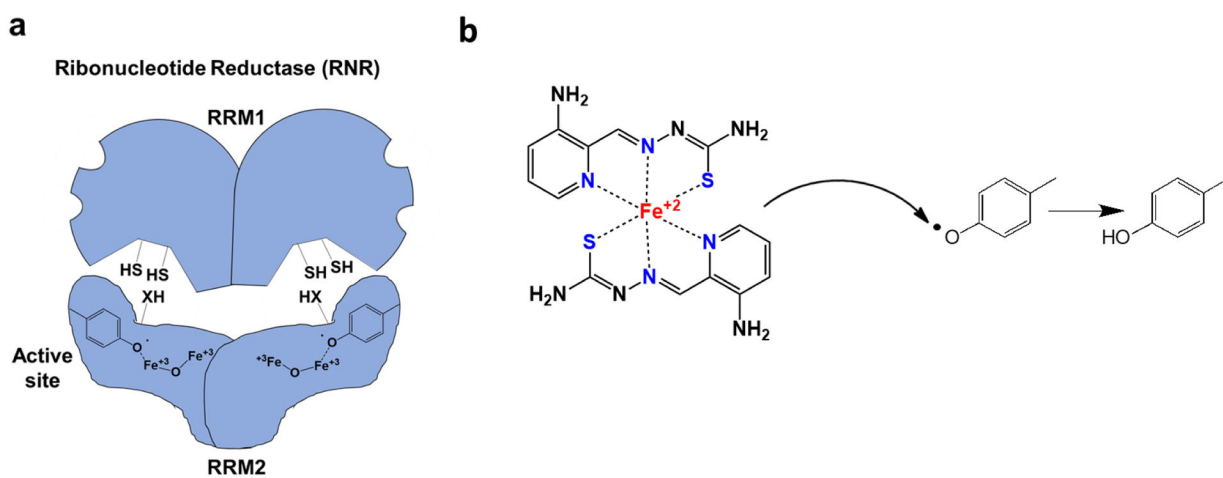
Figure 1.
(a) The catalytic subunit of human Ribonucleotide Reductase (RNR), contains a tyrosyl radical in the enzyme active site. (b) Fe(II) complexes of 3-AP and its analogs can quench the radical and, subsequently, inactivate RNR.
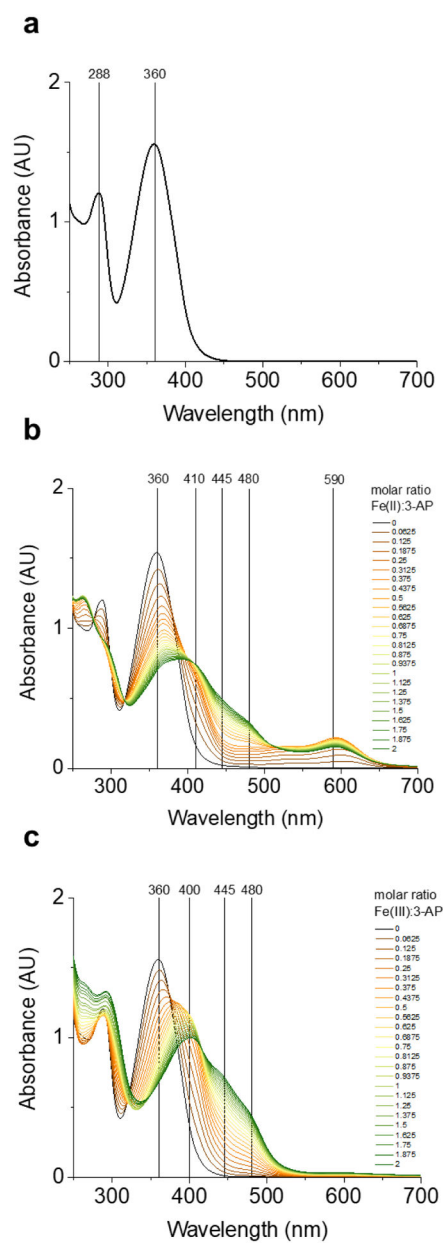
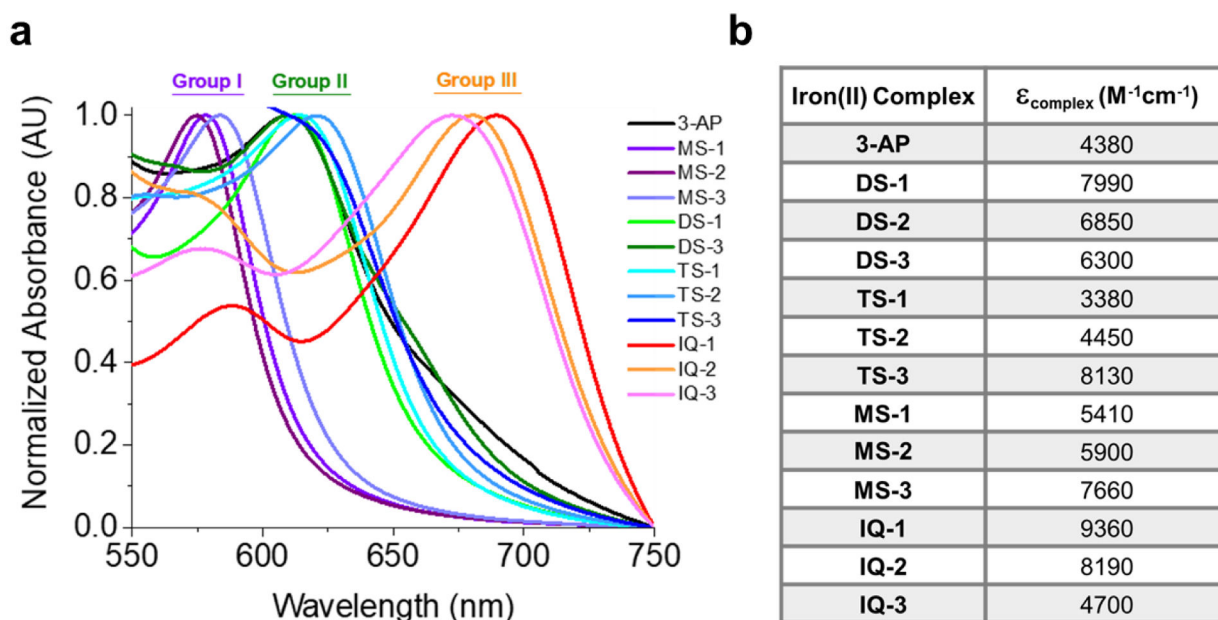**Figure 2.**
Structures of synthesized 3-AP analogs.

a

b

Drug	Minimum [drug] for S-phase arrest (uM)
IQ-1	0.25
DS-3	0.25
IQ-2	0.50
3-AP	0.50
DS-1	0.75
DS-2	0.75
IQ-3	1.50
TS-3	1.86
TS-2	3.75
TS-1	5.00
MS-1	No arrest (>5uM)
MS-2	No arrest (>5uM)
MS-3	No arrest (>5uM)

Figure 3.
(a) IC_{50} of 3-AP analogs in MIA PaCa-2 PDAC (pancreatic ductal adenocarcinoma) cells.
(b) Concentration at which S-phase arrest is induced (increase in population of S-phase cells by 20%) in MIA PaCa-2 cells by 3-AP analogs, determined by flow cytometry.

Figure 4.
(a) 3-AP free ligand in water, (b) 3-AP titrated with Fe(II), and (c) 3-AP titrated with Fe(III) to form the bis-complex.
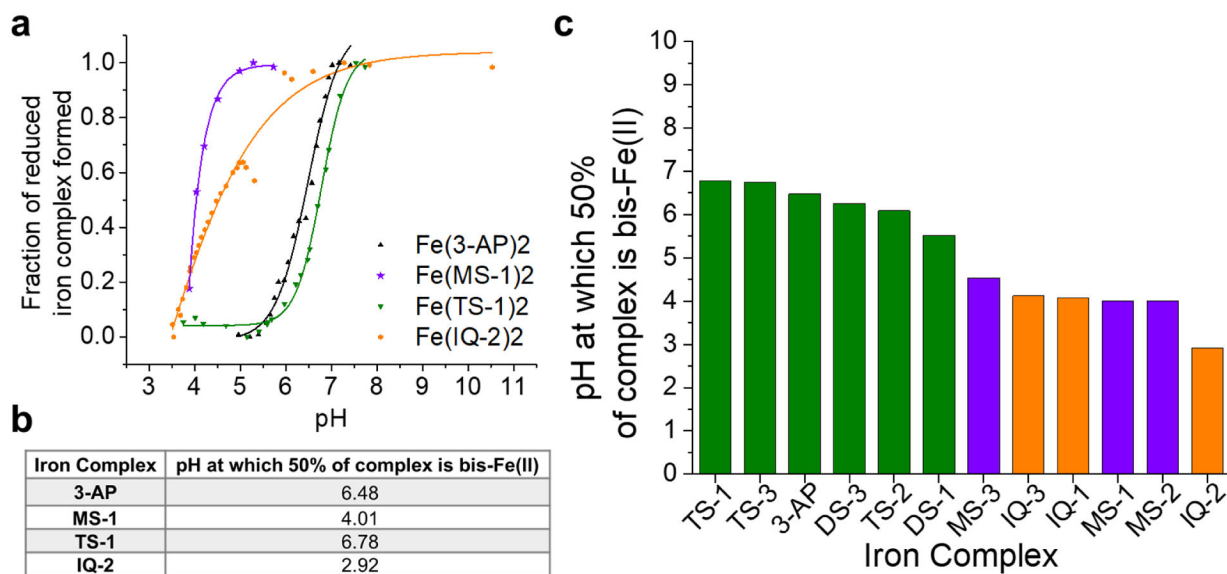
Figure 5.
(a) Bis-iron(II) complexes exhibit charge transfer peaks between 550 nm and 750 nm. Methylated Group I complexes are blue-shifted and isoquinoline Group III complexes are red-shifted, with respect to the 3-AP complex. (b) Extinction coefficients of the Fe(II) complexes at the lowest energy charge transfer transition wavelength.
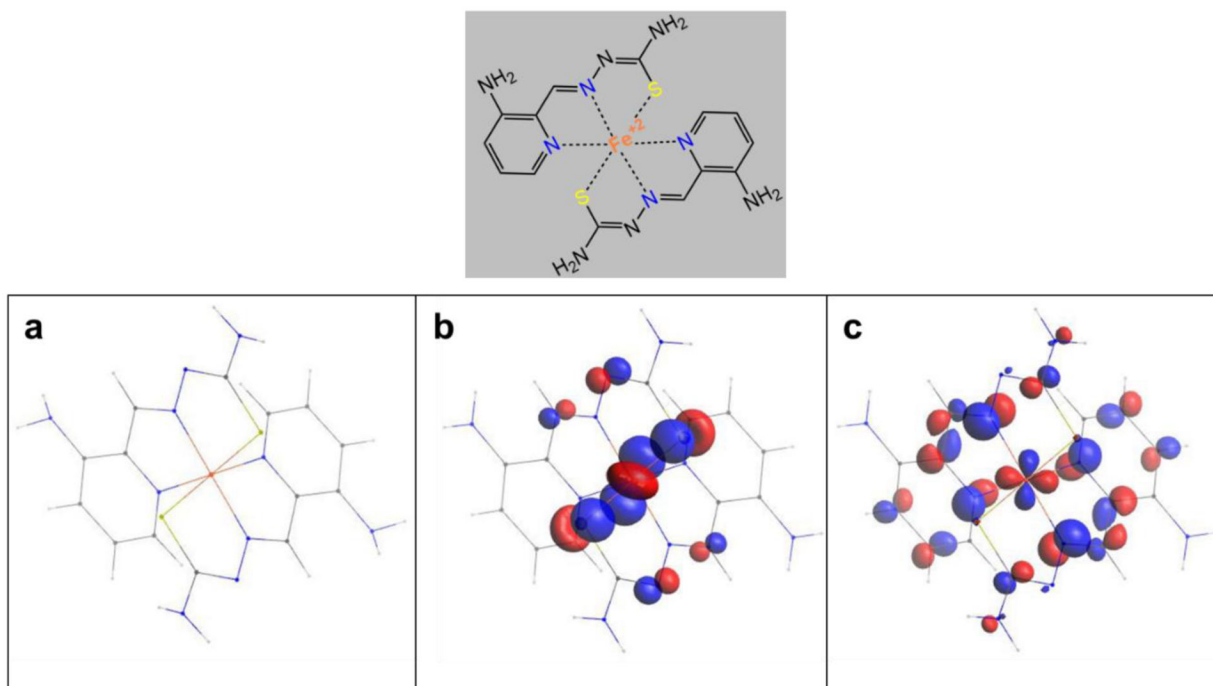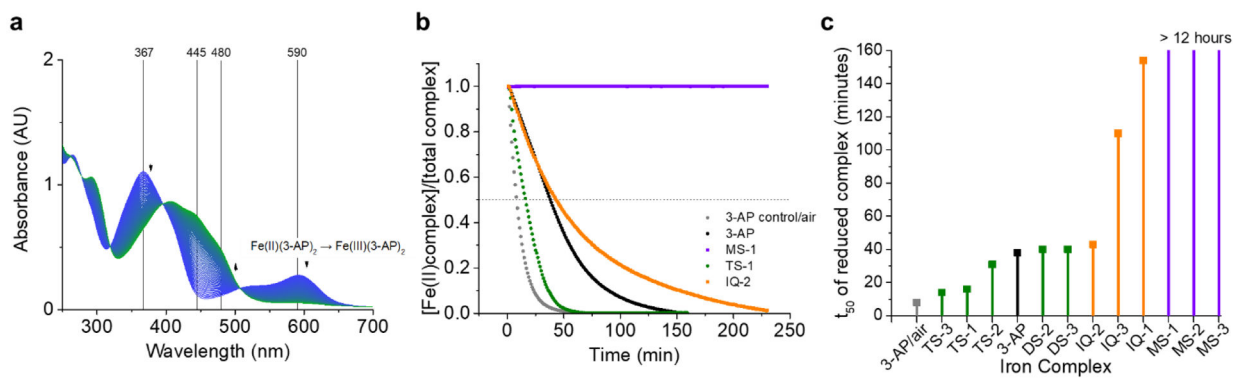
Figure 6.
(a) Optimized geometry from DFT calculations of the Fe(II)(3-AP)$_2$ octahedral complex starting from a previously published crystal structure [24]. (b) Calculated HOMO and (c) LUMO orbitals of Fe(II)(3-AP)$_2$ complex.
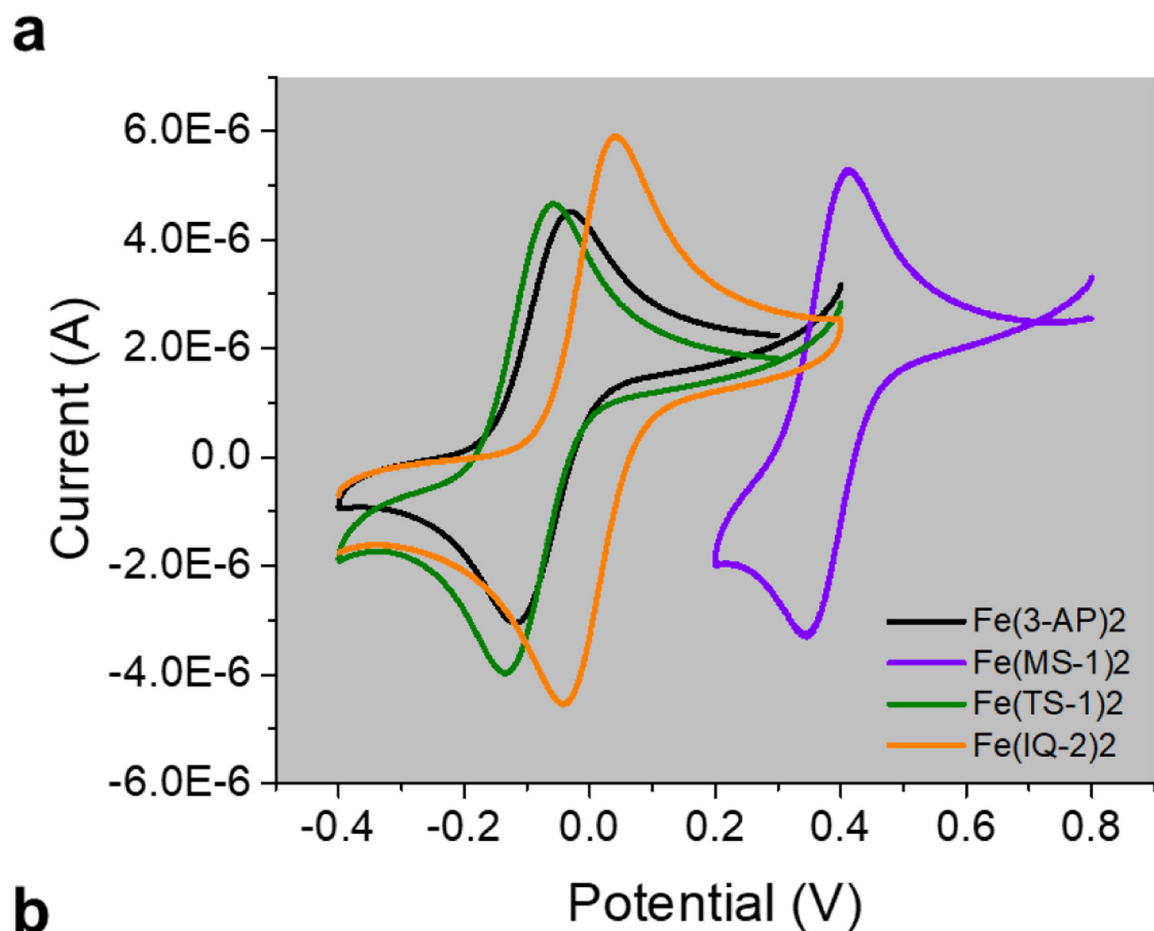
Figure 7.
(a) pH titrations of representative 3-AP iron (III) complexes in the presence of a reducing agent. The fraction of iron(II) complex formed is determined by UV-Vis from the absorbance of the lowest energy charge transfer peak. (b) Fraction of the active reduced species is plotted vs. pH and a sigmoidal curve fit is used to calculate the values in the table. (c) Summary of titration data for all the 3-AP analogs.
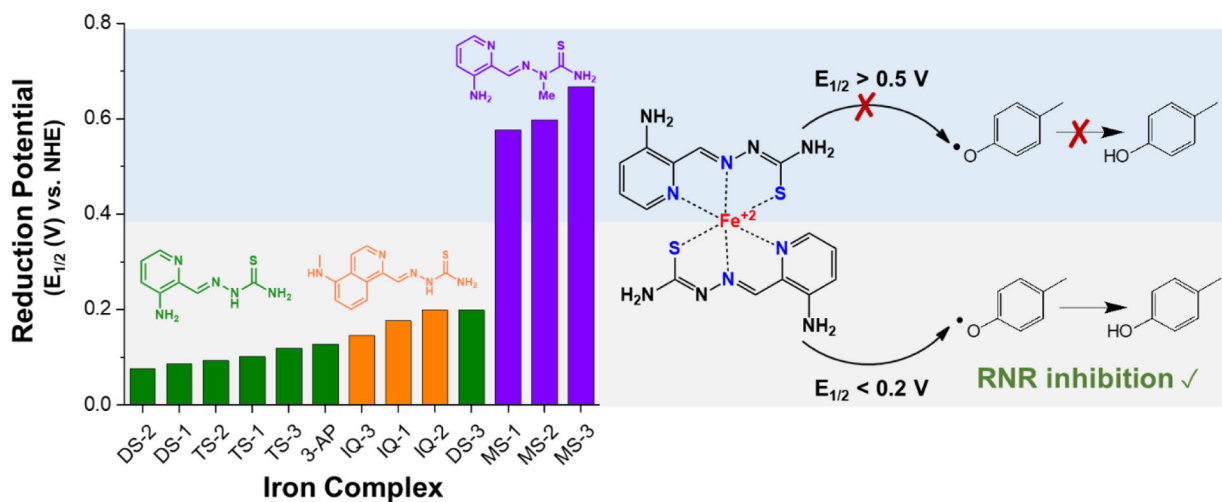
Figure 8.
(a) UV-Vis spectra for the oxidation of Fe(II)(3-AP)$_2$ over time, where absorption spectra are taken every 60 seconds. (b) Oxidation rate plotted as a function of absorbance of each 3-AP analog complex at the lowest energy charge transfer peak vs. time (c) Summary of t_{50} values for the 3-AP iron(II) complexes. T$_{50}$ is defined at the time it takes for 50% of the complex to get oxidized under the given experimental conditions.

Figure 9.
(a) Cyclic voltammograms of representative 3-AP analog complexes, (b) Reduction
potentials of complexes vs. Ag/AgCl and vs. NHE.

Figure 10.
Summary of redox potentials for all the iron complexes. Complexes that have redox potentials less than 0.2 V are able to redox cycle and inhibit RNR (grey region), while those that have redox potentials above 0.5 V are unable to be reduced in the cell and are thus inactive against RNR (blue region). Reduction potential, $E_{1/2}$, is expressed vs. NHE.